Heterogeneous Catalysis

Deutsche Ausgabe: DOI: 10.1002/ange.201704656
Internationale Ausgabe: DOI: 10.1002/anie.201704656

Controlling Reaction Selectivity through the Surface Termination of Perovskite Catalysts

*Felipe Polo-Garzon, Shi-Ze Yang, Victor Fung, Guo Shiou Foo, Elizabeth E. Bickel, Matthew F. Chisholm, De-en Jiang, and Zili Wu**

Abstract: *Although perovskites have been widely used in catalysis, tuning of their surface termination to control reaction selectivity has not been well established. In this study, we employed multiple surface-sensitive techniques to characterize the surface termination (one aspect of surface reconstruction) of $SrTiO_3$ (STO) after thermal pretreatment (Sr enrichment) and chemical etching (Ti enrichment). We show, by using the conversion of 2-propanol as a probe reaction, that the surface termination of STO can be controlled to greatly tune catalytic acid/base properties and consequently the reaction selectivity over a wide range, which is not possible with single-metal oxides, either SrO or TiO_2. Density functional theory (DFT) calculations explain well the selectivity tuning and reaction mechanism on STO with different surface termination. Similar catalytic tunability was also observed on $BaZrO_3$, thus highlighting the generality of the findings of this study.*

Perovskites are metal oxides with the general formula ABO_3, in which A represents a lanthanide, an alkali metal, or an alkaline earth metal and B represents a transition metal. The cations A and B can have a variety of oxidation states ($A^{+2}B^{+4}O_3$, $A^{+3}B^{+3}O_3$, and $A^{+1}B^{+5}O_3$). Also, the oxidation states can differ from the ideal structure, ABO_3, when the perovskite is oxygen-deficient or oxygen-rich.[1] These materials have shown high oxygen mobility, high tolerance for metal substitutions in the lattice structure, excellent thermal stability (up to 1000 °C), and resistance to sintering of substituted metals. These attributes have driven interest in perovskite materials, in particular for redox catalysis (e.g. methane reforming, CO oxidation, NO oxidation), whereas acid–base catalysis has yet to be extensively studied.[1,2] In the past five decades, researchers have unsuccessfully attempted to relate catalytic properties of bulk mixed oxides to bulk properties of the crystal structure, such as the short metal–oxygen bond. At the catalytic "stage", the surface of a complex oxide can be different from the bulk in both composition and structure, which has highlighted the need for surface-sensitive characterization of these materials to comprehend their catalytic behavior.[3] Surface-sensitive characterization is also needed for perovskites, in which surface reconstruction has been extensively observed in surface-science studies of single-crystal or thin-film forms. $SrTiO_3$ (STO) is among the most studied perovskites owing to its applications in catalysis,[4] its extensive use for the growth of important thin films, and its use as an insulating layer for potential field effect device applications and fundamental research.[5]

The surface reconstruction of STO has been found to be quite complex, depending on the treatment temperature, environment, and time. Also, these reconstructions have been shown to be reversible under certain conditions.[6] Druce et al.[7] and Ngai et al.[8] found A-cation enrichment at the surface after annealing perovskites in oxygen at 1000 °C for 12 h and at 1300 °C for 30 min, respectively. Dagdeviren et al.[6] and Nishimura et al.[9] reported Sr migration to the surface in STO and oxygen depletion during ultrahigh-vacuum (UHV) annealing. Contradictorily, Jiang and Zegenhagen[10] concluded that the SrO layer is less stable at high temperature (950–1100 °C), both in UHV and in oxygen. Erdman et al. studied the reconstruction of $SrTiO_3$ (001) and reported the formation of a single titanium-rich overlayer arranged as TiO_{6-x} polyhedra, in contrast to TiO_6 polyhedra in the bulk, after annealing under oxygen up to 1000 °C.[11] However, ab initio computational studies by Heifets et al.[12] do not support the (2×1) double-layer (DL) TiO_2-terminated surfaces observed by Erdman et al.[11b] This discrepancy reflects the complex dependence of the surface structure on the treatment conditions; furthermore, observed terminations could be due to kinetic processes far from thermodynamic equilibrium. Additionally, it was recently reported that the surface of STO can adopt the thin-film-like structure of octahedral titania,[13] thus highlighting the complexity of STO surface reconstruction.

Besides thermal treatment, chemical treatment under an acidic environment has been reported.[9,14] It has also been reported that Sr–O, Ti–O, and mixed terminations of STO nanoparticles depend upon the synthetic procedure;[15] however, their stability under reaction conditions for heterogeneous catalysis has not been reported.

The interaction of selected adsorbates (H_2O, NO, CO, CO_2, H_2, O)[16] with specific terminations of STO and other

[*] F. Polo-Garzon, G. S. Foo, Z. Wu
Chemical Sciences Division and Center for Nanophase Materials Sciences, Oak Ridge National Laboratory
Oak Ridge, TN 37831 (USA)
E-mail: wuz1@ornl.gov
S. Yang, M. F. Chisholm
Materials Science and Technology Division
Oak Ridge National Laboratory
Oak Ridge, TN 37831 (USA)
V. Fung, D. Jiang
Department of Chemistry, University of California
Riverside, CA 92521 (USA)
E. E. Bickel
Department of Chemical Engineering
Tennessee Technological University
Cookeville, TN 38505 (USA)
Supporting information and the ORCID identification number(s) for the author(s) of this article can be found under: https://doi.org/10.1002/anie.201704656.

perovskites has been examined. However, to the best of our knowledge, no comprehensive study on tuning reaction selectivity by controlling the surface termination of perovskite catalysts has been reported previously.

The present study successfully couples the surface terminations observed by top-surface sensitive characterization techniques with ab initio simulation and the catalytic performance of STO for the dehydrogenation/dehydration (acetone/propene production, respectively) of 2-propanol. During the thermal and chemical pretreatment of the samples, their crystal structure was conserved, as shown by X-ray diffraction (XRD; see Figure S1 in the Supporting Information).

Commercially obtained STO was thermally pretreated in situ in a plug-flow reactor at 550 °C under 5 % O_2/He (50 mL min^{-1}) for different time periods. After pretreatment, the conversion of 2-propanol at 303 °C was carried out in a plug-flow reactor (conversion $\leq$13 %). Longer pretreatment times greatly increased the rate of acetone production (dehydrogenation) from 0.15 to approximately 0.60 μmol m^{-2} min^{-1}, decreased the rate of propene production (dehydration) from approximately 0.32 to approximately 0.19 μmol m^{-2} min^{-1}, and therefore decreased the selectivity for the formation of propene (Figure 1 a). The possible role of different amounts of residual carbonates on STO after different pretreatment durations is excluded, as cofeeding CO_2 with 2-propanol did not change the catalytic performance of STO pretreated for 5 h (see Figure S2 a). It is thus hypothesized that longer pretreatment times favor the exposure of Sr atoms, since basic sites (predominant on a SrO surface termination, as shown in Figure S3 a,b) favor the dehydrogenation product, acetone.[17]

To test this hypothesis, we performed low-energy ion scattering (LEIS) characterization to determine the composition of the top atomic monolayer of the material (ca. 0.3 nm)[18] before and after thermal pretreatment. At the surface, STO presented a Sr-to-Ti ratio of around 0.7 before thermal pretreatment and 1.4 after thermal pretreatment at 500 °C in O_2 for 30 min (Figure 2 a), thus confirming the exposure of more Sr atoms upon thermal treatment at 500 °C under oxygen. Furthermore, it was observed that after thermal treatment for 4–5 h, the catalytic performance of STO did not change considerably. These results are in good agreement with the results reported by Bachelet et al.,[19] who showed that the SrO termination of STO substrates could be varied from 0 to 100 % when annealing at 1300 °C under air for different periods of time (2–72 h).

The conversion of 2-propanol at 300 °C was also evaluated on STO after in situ pretreatment at different temperatures for 5 h under 5 % O_2/He (50 mL min^{-1}; Figure 1 b). For pretreatment temperatures between 450 and 500 °C, the selectivity toward propene decreased significantly from 54 % at 450 °C to 31 % at 500 °C. However, for pretreatment temperatures above 500 °C the catalytic performance did not change. Thus, it was hypothesized that an increase in the pretreatment temperature exposes more Sr atoms at the surface but reaches a maximum for pretreatment temperatures above about 500 °C. When the thermally pretreated catalyst was held at room temperature for an extended period of time (at least for more than 2 weeks), the effect of thermal

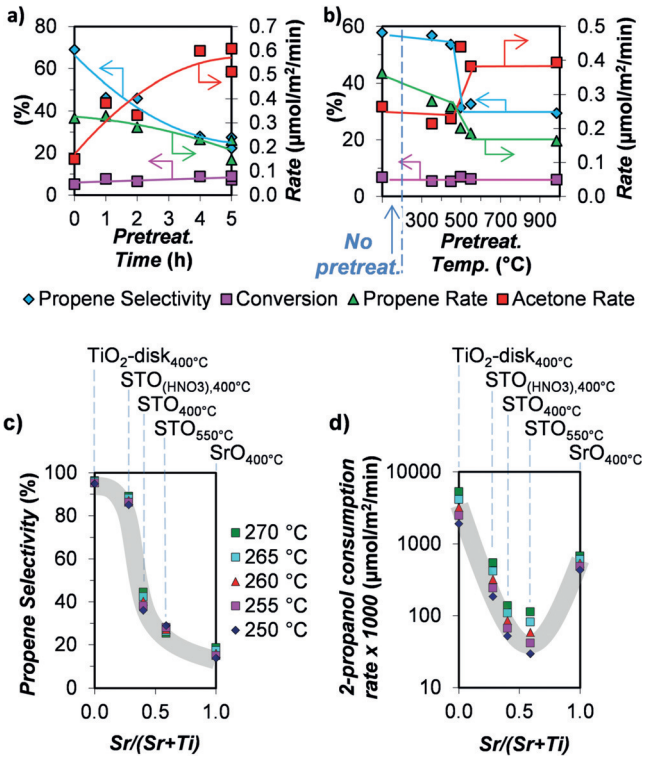

Figure 1. Steady-state conversion of 2-propanol a) at (303 ± 1) °C over STO after different pretreatment times at 550 °C under 5 % O_2/He (50 mL min^{-1}), and b) at (300 ± 1) °C after pretreatment at different temperatures under 5 % O_2/He (50 mL min^{-1}) for 5 h (1 h at 985 °C). c) Selectivity for the formation of propene and d) rate of consumption of 2-propanol (log scale) for the conversion of 2-propanol at 250–270 °C over $STO_{400°C}$, $STO_{550°C}$, $STO_{(HNO_3),400°C}$, TiO_2-$disk_{400°C}$, and $SrO_{400°C}$ catalysts. Reaction conditions: 50 mL min^{-1} Ar, 30 mg of catalyst, weight hourly space velocity (WHSV): 0.8 h^{-1}. The subscript next to the catalyst name indicates the pretreatment temperature under 5 % O_2/He (50 mL min^{-1}) for 5 h before kinetic data were collected.

a)

Catalyst	Sr/Ti
$STO_{(HNO3)}$	0.39
$STO_{(HNO3),500°C}$	0.48
STO	0.67
$STO_{500°C}$	1.44

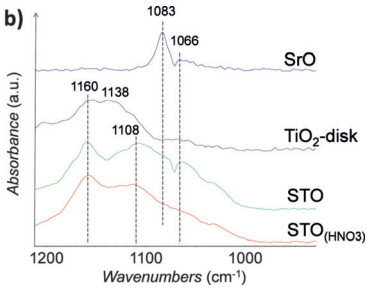

Figure 2. a) Top-surface Sr/Ti cation intensity ratio measured by LEIS for the pretreated STO and $STO_{(HNO_3)}$ catalysts. The subscript next to the catalyst name indicates the temperature at which the materials were pretreated in situ before LEIS analysis. b) FTIR spectra of methanol adsorption on SrO, TiO_2-disk, STO, and $STO_{(HNO_3)}$ catalysts at 25 °C. All samples were pretreated at 550 °C under oxygen.

pretreatment was reversed; that is, propene dominated over acetone as the product of the reaction of 2-propanol over such a sample. It appears that Sr exposure decreases upon the storage of STO at room temperature. This hypothesis was confirmed by LEIS analysis (Figure 2 a), which showed that the Sr-to-Ti ratio increased after treatment at 500 °C. How-

ever, this reverse process is not due to exposure to CO_2 or H_2O in the air, as confirmed experimentally (see Figure S2). The kinetics of the reverse process at room temperature, after thermal pretreatment, are interesting and warrant further investigation.

To promote the exposure of the Ti-terminated surface, we carried out ex situ pretreatment of STO in 0.2 M HNO_3 ($STO_{(HNO_3)}$) to remove the outmost SrO layer, as performed by Peng et al.[14a] on $La_{0.5}Sr_{0.5}CoO_3$. X-ray photoelectron spectroscopy (XPS) on $STO_{(HNO_3)}$ showed no remaining nitrogen (see Figure S4). Additionally, LEIS characterization (Figure 2a; see also Figures S5 and S6) confirmed the further exposure of Ti atoms after treatment with HNO_3 (Sr/Ti = 0.4), and it was found that thermal pretreatment of the washed sample, $STO_{(HNO_3),500\,°C}$, led to minor exposure of the Sr atoms (Sr/Ti = 0.5), far from the Sr exposure of the nonwashed thermally treated sample, $STO_{500\,°C}$ (Sr/Ti = 1.4).

We performed high-angle annular dark-field (HAADF) scanning transmission electron microscopy (STEM) on these differently treated STO samples to directly visualize the atomic structure of the surfaces. $STO_{(HNO_3)}$ was imaged after in situ heating at 400 °C under vacuum and after ex situ thermal pretreatment under N_2 at 550 °C for 5 h. STO was imaged before and after ex situ thermal pretreatment under N_2 at 550 °C for 5 h (see Figure 3). It was clearly observed that the surface of $STO_{(HNO_3)}$ was predominantly enriched with single and double layers of Ti. Also, heat treatment at 550 °C did not significantly affect the surface segregation of Ti for the chemically etched sample, which is in good agreement with LEIS results. The STO sample without heat treatment showed similar surface composition dominated by Ti but with the minor presence of Sr. However, surface enrichment with Sr was clearly observed upon heat treatment at 550 °C. For all STO samples, the (100) plane was confirmed as the main plane exposed at the surface with minor (110) truncation at the corners (see Figure S7 for a complete set of images); therefore, our DFT calculations were performed upon this major plane.

To study the relationship between the exposure of Sr/Ti atoms and the selectivity toward dehydrogenation/dehydration, we compared SrO (obtained commercially) and anatase TiO_2-disk (terminated by a large percentage with the (100) plane)[20] with pretreated STO samples. We carried out methanol adsorption followed by FTIR spectroscopy to compare the types of sites encountered in the strontium titanate samples with the sites in SrO and the TiO_2 disk (Figure 2b). Vibrational spectra of adsorbed methanol on both $STO_{550\,°C}$ and $STO_{(HNO_3),500\,°C}$ samples revealed spectral features resembling those present on both SrO and the TiO_2 disk, with $STO_{(HNO_3),500\,°C}$ closer to the TiO_2 disk and $STO_{550\,°C}$ closer to SrO, thus further supporting the surface enrichment as analyzed by LEIS and STEM. The observation of different methanol species on both STO samples suggests a synergistic effect arising from the coexistence of Sr and Ti at the surface (see the Supporting Information for details). To quantify the concentration and strength of basic and acid sites, adsorption microcalorimetry measurements were performed with CO_2 and NH_3, respectively. In general, the result showed that $STO_{550\,°C}$ has more basic sites but fewer acidic sites when compared with $STO_{(HNO_3),500\,°C}$ (see Figure S3a,b), which is consistent with the higher Sr/Ti ratio on the former STO sample. Nonetheless, the strength (see Figure S3a,b) of the basic or acid sites approaching zero surface coverage does not directly correlate with the density of the sites ($\mu mol\,m^{-2}$; see Table S3 in the Supporting Information) or with the fraction of Sr at the outermost layer [Sr/(Sr + Ti)] (see Table S3). This synergistic effect can be explained by the presence of Sr–O or Ti–O sublayers that together tune the basic/acid properties of the surface (see the Supporting Information for further details).

The heat of adsorption of 2-propanol was also measured. Noticeably, the adsorption strength of 2-propanol did not vary significantly for three of the samples studied (STO, $STO_{(HNO_3)}$, and the TiO_2 disk), thus suggesting that the adsorption strength of 2-propanol is similar at Ti and Sr sites, except when more than one SrO layer is stacked at the surface, as in the case of the pure SrO catalyst (on which CO_2 adsorption may involve a reaction to form $SrCO_3$). DFT calculations revealed dissociative adsorption of 2-propanol on the Sr-terminated surface and chemisorption that readily leads to dissociation on the Ti-terminated surface. On the Ti-terminated surface, the reaction energy (ΔH_{rxn}) for the dissociation of 2-propanol and the corresponding activation barrier

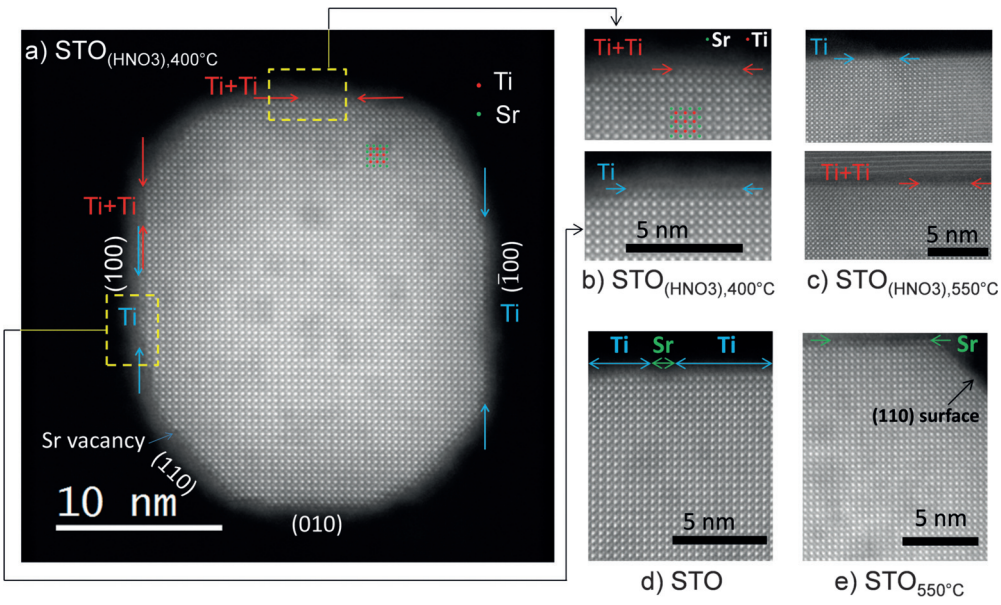

Figure 3. HAADF STEM images of $STO_{(HNO_3)}$ after heat treatment at a,b) 400 °C and c) 550 °C, as well as images of STO d) before and e) after heat treatment at 550 °C.

(ΔE_{act}) are −0.33 and 0.18 eV, respectively. The calculated adsorption energies for dissociated 2-propanol on Sr- and Ti-terminated surfaces of STO were 135 and 112 kJ mol^{-1}, respectively (see Figures S8–S12), thus setting the boundary for the strongest adsorption energy (at coverage approaching zero) of 2-propanol on the STO catalyst, on which both Sr- and Ti-terminated surfaces are present. This range (between 135 and 112 kJ mol^{-1}) is in good agreement with the experimental values ranging from 110 to 103 kJ mol^{-1} (see Figure S3 c).

To further understand our experimental observation of the selectivity changes upon different conditioning of STO, we used DFT to probe the reaction pathways of 2-propanol on the Ti- and Sr-terminated STO (100) surfaces. These surfaces are a simplified version of the more complicated real surfaces; therefore, they are used to shed light on reactivity trends, and comparisons with experimental results are rather qualitative. The results suggest that both dehydrogenation and dehydration of 2-propanol involve initial deprotonation to generate the 2-propanoxy intermediate; then, depending upon the basicity of the adjacent surface oxygen atom, either the C_β–H or C_α–H bond is cleaved to produce propene or acetone, respectively (see the Supporting Information). This reaction mechanism is denoted as the E_{1cB} pathway and is expected from the weak acidity of the surface sites in STO.[21] The rate-determining step (RDS) for acetone formation is the cleavage of the C_α–H bond and for propene formation is the concerted cleavage of the C_β–H and C–O bonds (Figure 4). Calculations show that the Ti-terminated surface of STO favors the production of propene ($\Delta E_{a,propene} = 145$ kJ mol^{-1}, $\Delta E_{a,acetone} = 155$ kJ mol^{-1}) and the Sr-terminated surface favors the production of acetone ($\Delta E_{a,propene} = 235$ kJ mol^{-1}, $\Delta E_{a,acetone} = 149$ kJ mol^{-1}), which agrees well with our experimental observations.

Apparent activation energies were calculated by fitting the Arrhenius equation to kinetic data (see Figure S13 and Table S4) collected under differential conditions (conversion $\leq 13\,\%$)[21] and used to compare reactivity data at the same temperature for the five samples: TiO_2-disk$_{400\,°C}$, $SrO_{400\,°C}$, $STO_{(HNO_3),400\,°C}$, $STO_{400\,°C}$, and $STO_{550\,°C}$. Apparent activation energies for acetone production on surface-Sr-rich STO ($STO_{550\,°C}$; 163 kJ mol^{-1}) and for propene production on a surface-Ti-rich STO sample ($STO_{(HNO_3),400\,°C}$; 130 kJ mol^{-1}) showed general agreement with the magnitude of the DFT-calculated activation energies for the RDS, namely, 149 and 145 kJ mol^{-1}, respectively. Although the good agreement between our DFT barriers of the rate-limiting steps and the experimental apparent activation energies sheds light on the reaction mechanisms at the two different terminations, a proper reaction kinetic analysis is warranted in the future to firmly establish a relationship between the DFT-predicted mechanism and the experimental kinetic data.

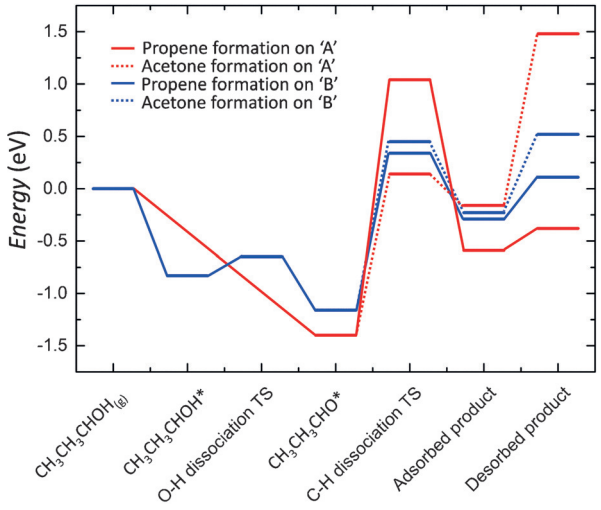

Figure 4. Minimum-energy paths for the conversion of 2-propanol over Sr-terminated (A) and Ti-terminated surfaces (B) of STO(100) into propene and acetone.

The unique tunability of reaction selectivity through induced surface terminations of STO is evident from a comparison with the individual single oxides. As seen in Figure 1 c, in the range 250–270 °C, TiO_2-disk$_{400\,°C}$ and $SrO_{400\,°C}$ showed around 95 and 15 % selectivity for the formation of propene, respectively. The perovskite samples enabled propene selectivities of 25 to 87 % to be reached by tuning their surface composition. Figure 1 d suggests that the coexistence of Sr and Ti atoms at the surface with a composition of around 28–59 % Sr induces lower rates of both dehydrogenation and dehydration. Since deprotonation of the 2-propoxy intermediate is assisted by a nearby surface oxygen atom, for a mixed Sr–Ti surface with different basicities, protonation/deprotonation processes may occur simultaneously, which is reflected by a reduction in the rate of 2-propanol consumption for STO catalysts. Also, adsorption microcalorimetry measurements suggest that subsurface layers may tune the acidity and basicity of the surface (see the Supporting Information for details), which can potentially interfere with the rate of protonation/deprotonation. Despite the decrease in the reaction rate, perovskite catalysts enable the ratio of dehydrogenation and dehydration rates to be controlled owing to the synergy between acid and base sites, as observed through FTIR spectroscopy and adsorption microcalorimetry experiments.

In conclusion, we have shown by using the conversion of 2-propanol as a probe reaction that altering the surface termination of $SrTiO_3$ enables its acid/base catalytic properties to be tuned, thus providing selectivities that are inaccessible with the single-metal oxides, namely, SrO and TiO_2. Controlled enrichment of Sr or Ti at the surface of $SrTiO_3$ by thermal and chemical treatment was revealed by LEIS and HAADF STEM. Methanol adsorption followed by FTIR spectroscopy and adsorption microcalorimetry measurements revealed the synergistic nature of the surface Sr and Ti sites for 2-propanol conversion. DFT calculations were in good agreement with the experimental data and showed that both the dehydrogenation and dehydration pathways proceed via the 2-propoxy intermediate. Furthermore, extension to $BaZrO_3$ (see Figure S15) suggests that the potential of inducing the surface termination of perovskites to control catalytic selectivity is general. The findings of this study have significant implication for catalysis by mixed oxides, the surface and bulk compositions of which can be different depending on treatment and reaction conditions. Advantage has yet to be taken of modifying the surface termination of these materials as a unique route to tune their

catalytic performance. Our findings also underscore the importance and necessity of the surface-sensitive characterization of bulk mixed oxides (prior to and after reaction, ideally under the reaction conditions) for unambiguous structure–catalysis correlation.

Acknowledgements

This research was sponsored by the U.S. Department of Energy, Office of Science, Office of Basic Energy Sciences, Chemical Sciences, Geosciences, and Biosciences Division. Part of the research, including FTIR, BET, and kinetic measurements, was conducted at the Center for Nanophase Materials Sciences, which is a DOE Office of Science User Facility. This research used resources of the National Energy Research Scientific Computing Center, a DOE Office of Science User Facility supported by the Office of Science of the U.S. Department of Energy under Contract No. DE-AC02-05CH11231. Electron microscopy at Oak Ridge National Laboratory (S.-Z.Y. and M.F.C.) was supported by the U.S. Department of Energy, Office of Science, Basic Energy Sciences, Materials Science and Engineering Division. We thank Henry Luftman (Lehigh University) for performing the LEIS analysis and Zach Hood (graduate student at Georgia Institute of Technology) for performing XPS measurements.

Conflict of interest

The authors declare no conflict of interest.

Keywords: acid/base catalysis · dehydration/dehydrogenation · heterogeneous catalysis · perovskites · surface termination

How to cite: *Angew. Chem. Int. Ed.* **2017**, *56*, 9820–9824
Angew. Chem. **2017**, *129*, 9952–9956

[1] a) S. Royer, D. Duprez, F. Can, X. Courtois, C. Batiot-Dupeyrat, S. Laassiri, H. Alamdari, *Chem. Rev.* **2014**, *114*, 10292–10368; b) H. Zhu, P. Zhang, S. Dai, *ACS Catal.* **2015**, *5*, 6370–6385.

[2] D. Pakhare, J. Spivey, *Chem. Soc. Rev.* **2014**, *43*, 7813–7837.

[3] a) I. E. Wachs, K. Routray, *ACS Catal.* **2012**, *2*, 1235–1246; b) S. V. Merzlikin, N. N. Tolkachev, L. E. Briand, T. Strunskus, C. Wöll, I. E. Wachs, W. Grünert, *Angew. Chem. Int. Ed.* **2010**, *49*, 8037–8041; *Angew. Chem.* **2010**, *122*, 8212–8216.

[4] a) J. M. P. Martirez, S. Kim, E. H. Morales, B. T. Diroll, M. Cargnello, T. R. Gordon, C. B. Murray, D. A. Bonnell, A. M. Rappe, *J. Am. Chem. Soc.* **2015**, *137*, 2939–2947; b) J. G. Mavroides, J. A. Kafalas, D. F. Kolesar, *Appl. Phys. Lett.* **1976**, *28*, 241–243; c) R. Konta, T. Ishii, H. Kato, A. Kudo, *J. Phys. Chem. B* **2004**, *108*, 8992–8995; d) K. Iwashina, A. Kudo, *J. Am. Chem. Soc.* **2011**, *133*, 13272–13275; e) J. W. Liu, G. Chen, Z. H. Li, Z. G. Zhang, *J. Solid State Chem.* **2006**, *179*, 3704–3708.

[5] a) C. Aruta, J. Zegenhagen, B. Cowie, G. Balestrino, G. Pasquini, P. G. Medaglia, F. Ricci, D. Luebbert, T. Baumbach, E. Riedo, L. Ortega, R. Kremer, J. Albrecht, *Phys. Status Solidi A* **2001**, *183*, 353–364; b) R. Droopad, Z. Yu, J. Ramdani, L. Hilt, J. Curless, C. Overgaard, J. L. Edwards, Jr., J. Finder, K. Eisenbeiser, W. Ooms, *Mater. Sci. Eng. B* **2001**, *87*, 292–296; c) X. X. Xi, Q. Li, C. Doughty, C. Kwon, S. Bhattacharya, A. T. Findikoglu, T. Venkatesan, *Appl. Phys. Lett.* **1991**, *59*, 3470–3472.

[6] O. E. Dagdeviren, G. H. Simon, K. Zou, F. J. Walker, C. Ahn, E. I. Altman, U. D. Schwarz, *Phys. Rev. B* **2016**, *93*, 195303.

[7] J. Druce, H. Tellez, M. Burriel, M. D. Sharp, L. J. Fawcett, S. N. Cook, D. S. McPhail, T. Ishihara, H. H. Brongersma, J. A. Kilner, *Energy Environ. Sci.* **2014**, *7*, 3593–3599.

[8] J. H. Ngai, T. C. Schwendemann, A. E. Walker, Y. Segal, F. J. Walker, E. I. Altman, C. H. Ahn, *Adv. Mater.* **2010**, *22*, 2945–2948.

[9] T. Nishimura, A. Ikeda, H. Namba, T. Morishita, Y. Kido, *Surf. Sci.* **1999**, *421*, 273–278.

[10] Q. D. Jiang, J. Zegenhagen, *Surf. Sci.* **1999**, *425*, 343–354.

[11] a) N. Erdman, O. Warschkow, M. Asta, K. R. Poeppelmeier, D. E. Ellis, L. D. Marks, *J. Am. Chem. Soc.* **2003**, *125*, 10050–10056; b) N. Erdman, K. R. Poeppelmeier, M. Asta, O. Warschkow, D. E. Ellis, L. D. Marks, *Nature* **2002**, *419*, 55–58.

[12] E. Heifets, S. Piskunov, E. A. Kotomin, Y. F. Zhukovskii, D. E. Ellis, *Phys. Rev. B* **2007**, *75*, 115417.

[13] Z. Wang, A. Loon, A. Subramanian, S. Gerhold, E. McDermott, J. A. Enterkin, M. Hieckel, B. C. Russell, R. J. Green, A. Moewes, J. Guo, P. Blaha, M. R. Castell, U. Diebold, L. D. Marks, *Nano Lett.* **2016**, *16*, 2407–2412.

[14] a) Y. Peng, W. Si, J. Luo, W. Su, H. Chang, J. Li, J. Hao, J. Crittenden, *Environ. Sci. Technol.* **2016**, *50*, 6442–6448; b) L. C. Seitz, C. F. Dickens, K. Nishio, Y. Hikita, J. Montoya, A. Doyle, C. Kirk, A. Vojvodic, H. Y. Hwang, J. K. Norskov, T. F. Jaramillo, *Science* **2016**, *353*, 1011–1014.

[15] Y. Lin, J. Wen, L. Hu, R. M. Kennedy, P. C. Stair, K. R. Poeppelmeier, L. D. Marks, *Phys. Rev. Lett.* **2013**, *111*, 156101.

[16] a) Z. M. Wang, X. F. Hao, S. Gerhold, Z. Novotny, C. Franchini, E. McDermott, K. Schulte, M. Schmid, U. Diebold, *J. Phys. Chem. C* **2013**, *117*, 26060–26069; b) R. A. Evarestov, A. V. Bandura, V. E. Alexandrov, *Surf. Sci.* **2007**, *601*, 1844–1856; c) H. J. Zhang, G. Chen, Z. H. Li, *Appl. Surf. Sci.* **2007**, *253*, 8345–8351; d) J. A. Rodriguez, S. Azad, L. Q. Wang, J. Garcia, A. Etxeberria, L. Gonzalez, *J. Chem. Phys.* **2003**, *118*, 6562–6571; e) S. Azad, M. H. Engelhard, L.-Q. Wang, *J. Phys. Chem. B* **2005**, *109*, 10327–10331; f) Ref. [4a]; g) B. Stöger, M. Hieckel, F. Mittendorfer, Z. Wang, D. Fobes, J. Peng, Z. Mao, M. Schmid, J. Redinger, U. Diebold, *Phys. Rev. Lett.* **2014**, *113*, 116101; h) R. Hammami, H. Batis, C. Minot, *Surf. Sci.* **2009**, *603*, 3057–3067; i) K. A. Stoerzinger, R. Comes, S. R. Spurgeon, S. Thevuthasan, K. Ihm, E. J. Crumlin, S. A. Chambers, *J. Phys. Chem. Lett.* **2017**, *8*, 1038–1043; j) A. V. Bandura, R. A. Evarestov, D. D. Kuruch, *Surf. Sci.* **2010**, *604*, 1591–1597; k) R. A. Evarestov, A. V. Bandura, E. N. Blokhin, *J. Phys. Conf. Ser.* **2007**, *93*, 012001; l) K. A. Stoerzinger, W. T. Hong, E. J. Crumlin, H. Bluhm, M. D. Biegalski, Y. Shao-Horn, *J. Phys. Chem. C* **2014**, *118*, 19733–19741; m) H. Kizaki, K. Kusakabe, *Surf. Sci.* **2012**, *606*, 337–343; n) I. W. Boateng, R. Tia, E. Adei, N. Y. Dzade, C. R. A. Catlow, N. H. De Leeuw, *Phys. Chem. Chem. Phys.* **2017**, *19*, 7399–7409; o) G. Pilania, R. Ramprasad, *Surf. Sci.* **2010**, *604*, 1889–1893.

[17] G. Tesquet, J. Faye, F. Hosoglu, A.-S. Mamede, F. Dumeignil, M. Capron, *Appl. Catal. A* **2016**, *511*, 141–148.

[18] a) H. R. J. ter Veen, T. Kim, I. E. Wachs, H. H. Brongersma, *Catal. Today* **2009**, *140*, 197–201; b) S. P. Phivilay, A. A. Puretzky, K. Domen, I. E. Wachs, *ACS Catal.* **2013**, *3*, 2920–2929.

[19] R. Bachelet, F. Sánchez, F. J. Palomares, C. Ocal, J. Fontcuberta, *Appl. Phys. Lett.* **2009**, *95*, 141915.

[20] J. Liu, D. Olds, R. Peng, L. Yu, G. S. Foo, S. Qian, J. Keum, B. Gui-ton, Z. Wu, K. Page, *Chem. Mater.* **2017**, *29*, 5591–5604.

[21] G. S. Foo, F. Polo-Garzon, V. Fung, D.-e. Jiang, S. H. Overbury, Z. Wu, *ACS Catal.* **2017**, *7*, 4423–4434.

Manuscript received: May 5, 2017
Accepted manuscript online: June 21, 2017
Version of record online: July 19, 2017

